DOI: 10.26599/FSHW.2024.9250393



Contents lists available at SciOpen

Food Science and Human Wellness

journal homepage: https://www.sciopen.com/journal/2097-0765

# The impact of Cistanche on the therapeutic potential of acne after fermentation with *Beauveria bassiana*.

Xingjiang Zhang[1], Pan Wang[1], Yunwei Hu[1], Hui Ke[1], Rui Wang[1], Xiaoya Zhang[1], Huiyun Wu[1], Baiyi Chi[1], Yuyo Go[2], Xi Hui Felicia Chan[3], Qing Huang[1]*, Jianxin Wu[1]*

[1]*Skin Health and Cosmetic Development & Evaluation Laboratory, China Pharmaceutical University, Nanjing 211198 Jiangsu, China*

[2]*Royal Victoria Hospital, 274 Grosvenor Rd, Belfast BT12 6BA, United Kingdom;*

[3]*Acute Mental Health Inpatient Centre, Belfast, BT9 7YG, United Kingdom;*

**ABSTRACT:** Phenylethanol glycosides (PhGs) constitute crucial bioactive compounds in Cistanche Herba. However, their bioavailability is notably low. Research indicates that intestinal flora can metabolize PhGs into small polyphenols, enhancing bioavailability and pharmacological activities. In this paper, for the first time, a single strain, *Beauveria bassiana*, was found to be effective in converting PhGs from the crude extract of *Cistanche tubulosa* into small molecule polyphenols like hydroxytyrosol (HT), decaffeoylacteoside (HT-rha-glu), and caffeic acid through fermentation. We assessed the impact of pre- and post-fermentation on *Propionibacterium acnes* (*P. acnes*)-induced acne related to a western diet through *in vitro* cellular experiments. Both pre- and post-fermentation exhibited efficacy in inhibiting inflammation, oxidative stress, and mitochondrial membrane damage in *P. acnes*-induced HaCaT. Moreover, post-fermentation, unlike pre-fermentation, displayed stronger and a dose-dependent reduction in insulin-stimulated lipid synthesis in sebaceous gland cells. To further understand the increased efficacy of fermentation in inhibiting lipid synthesis, we investigated HT-rha-glu, the predominant small molecules produced during fermentation. It was shown that the compound inhibited lipid synthesis by decreasing gene expression of SREBP-1 and PPARγ in sebaceous gland cells.

**Keywords:** Cistanche; fermentation; *Beauveria bassiana*; acne; decaffeoylacteoside

## 1. Introduction

Cistanche Herba is a parasitic plant thriving in arid regions across Asia and Africa. With a long history in traditional Chinese medicine, it has served as a tonic and aphrodisiac for centuries. This herb is widely embraced as a health food supplement in Japan, China, and several Southeast Asian nations[1].

Cistanche Herba and its phenylethanol glycosides (PhGs) have been reported to exhibit various pharmacological effects, such as neuroprotection[2], immune regulation[3], antiaging[4], anti-osteoporosis[5], liver protection[6], etc. Among the PhGs, echinacoside are the most abundant and studied compounds in *Cistanche tubulosa*[7]. However, one of the major challenges of using echinacoside as oral drugs is their low bioavailability. A previous pharmacokinetic study showed that the absolute bioavailability (F, %) of

***Corresponding author**
wujianxin@cpu.edu.cn; huangqing@cpu.edu.cn

Received 8 April 2024
Received in revised from 21 April 2024
Accepted 23 September 2024

echinacoside was only 0.83%[8]. This means that only a small fraction of the ingested echinacoside can reach the systemic circulation and exert their pharmacological effects. It is well known that prior to being absorbed into blood, many oral drugs are transformed by intestinal bacteria in gastrointestinal tract[9]. These gut flora play a key role in the digestive process, and some of them have the ability to metabolize PhGs into smaller compounds that are more easily absorbed[10]. For instance, echinacoside, when metabolized by intestinal bacteria, breaks down into smaller compounds such as hydroxytyrosol (HT), caffeic acid, verbascoside, and decaffeoylacteoside (HT-rha-glu)[11]. These metabolites exhibit enhanced biological activity compared and bioavailability to their parent compounds[12]. This could elucidate why echinacoside presents low absolute bioavailability but demonstrates notable biological activity. Therefore, *in vitro* microbial transformation of PhGs to improve their bioavailability and pharmacological activity deserves further study.

Fermented foods or medicinal materials have higher efficacy and utilization than unfermented ones. Fermentation can deglycosylate some glycosidic compounds, making them into smaller, more absorbable, and more permeable non-glycosidic compounds[13]. For instance, lactic acid bacteria (*Lactiplantibacillus plantarum*) has the capacity to transform relatively less biologically active flavonoid glycosides such as hesperidin and naringin into more active aglycones, namely hesperetin and naringenin. Both *in vitro* and *in vivo* studies have demonstrated the enhanced cellular transport and increased bioactivity of the fermented citrus extract[14].

*Beauveria bassiana* is a medicinal fungus that grows on silkworm carcasses. For centuries, infected silkworms have been utilized in Asian medicine as a tonic and immunomodulator, and was described in "Sheng Nong's herbal classic"[15]. *B. bassiana* is generally considered safe for humans, animals, and other non-target organisms[16] and performs efficient biotransformation of natural compounds and xenobiotics[17]. Recent human exposure risk assessments of some of its metabolites have further confirmed its safety for human use[18]. A blend of plant extracts underwent fermentation by *B. bassiana* and was evaluated for its impact on chicken embryo blood vessels. The fermentation process transformed Glucogallin into Gallic acid within the mixture, resulting in reduced toxicity and enhanced antiangiogenic properties[19].

In this study, we found for the first time that a single strain of *B. bassiana* can biotransform PhGs into small molecule polyphenols, whereas most of the previous studies have focused on the transformation of PhGs in intestinal flora. Moreover, the transformation of *B. bassiana* is similar to the metabolites produced by PhGs in human metabolism and intestinal flora, and has the potential for large-scale fermentation production. We used the fermentation product in the treatment of acne and showed good therapeutic potential *in vitro*. It provides a theoretical basis for the use of Cistanche herbs in beauty and skin care.

## 2. Materials and methods

### *2.1 Materials and chemicals*

The crude extract from *Cistanche tubulosa* was provided by Prof. *** of Peking University (Beijing, China). The extraction and purification process are broadly as follows: fifty grams of the sample was

weighed and reflux extracted twice, each for 1 hour, with 600 mL of 70% ethanol. Dynamic adsorption was performed using HPD-100 resin, and the sample was eluted with a 50% ethanol solution. After recovering the ethanol under reduced pressure, the dried powder was obtained by freeze-drying using a freeze-dryer. HT, caffeic acid, verbascoside, isoacteoside and HT-rha-glu, all with the purity of over 98% were purchased from Chengdu Push Bio-technology Co., Ltd (Sichuan, China). *B. bassiana* were obtained from China Center of Industrial Culture Collection CICC (Beijing, China). Insulin was procured from Solarbio Life Sciences (Beijing, China), and Cell Counting Kit-8 (CCK-8) was obtained from Vazyme (Nanjing, China).

*2.2 Fermentation and sample collection*

Inoculate the *B. bassiana* into Shah's glucose liquid medium under aseptic condition, and cultivate it under 28℃ condition with 200 r/min shaking bed for 2 days to make the first-grade seeds, and the OD600 value of the optical density of *B. bassiana* suspension at the end of the cultivation reaches about 0.8; Secondary seed culture: according to the volume ratio of Shah's glucose liquid medium for 10% of the inoculum, the first level of seed inoculation into the 200 mL conical flask at 28℃, stirring speed of 200 r/min, culture for 2 days, to produce the second level of seed; Put 0.3 g crude extract from *Cistanche tubulosa* into 200 mL secondary seed liquid, and incubate at 28℃ with stirring speed of 200 r/min. Among these, BJJ (*B. bassiana* alone for 12 days in medium without crude extract), BJJF (*B. bassiana* in medium containing crude extract for 12 days), and PHG (crude extract dissolved in medium without *B. bassiana*).

*2.3 Qualitative LC-MS/MS analysis*

The compounds in the crude extracts before and after fermentation were characterized using a Waters ACQUITY UPLC I-CLASS Plus/Xeve G2-XS Q TOF instrument. This instrument incorporated a Waters ACQUITY UPLC BEH-C18 column (2.1 mm, 100 mm, 1.8 μm) and a mobile phase consisting of two constituents: 0.1% formic acid (FA) in water (A) and 0.1% FA in acetonitrile (ACN) (B). Operating at a flow rate of 0.3 mL/min, the column was maintained at a temperature of 40℃, while the sample chamber temperature was regulated at 4℃. Samples were detected by absorption with a wavelength range of 190-400 nm, with an inject volume of 5 μL.

The mobile phase was programmed as follows: an isocratic elution of 2%-4% B for the first 5 min, followed by a linear gradient elution of 4%-13% B from 5 to 8.5 min, 13%-18% B from 8.5 to 10 min, 18% B from 10 to 12 min, 18%-40% B from 12 to 15 min, 40%-100% B from 15 to 15.5 min. After holding the solvent composition of 100% B for the next 2 min, the gradient was returned to its starting conditions.

Mass spectrometry analysis was performed using two ionization modes: electron source ionization ($ESI^+$) and electron capture source ionization ($ESI^-$). A source voltage of 3.0 kV and a source temperature of 450℃ were applied to generate ions in both modes. An acquisition mass range of 50 to 1200 Da was utilized. A cone voltage of 50 L/Hr and an acquisition time of around one second per spectrum were employed during the analysis. After the data acquisition using Q-TOF, the raw data were imported and processed (peak alignment, detection and identification) using the MSDIAL software system. The software determined the retention time and m/z data for each peak.

*2.4 Quantitative LC-UV analysis*

LC experiments were conducted using a Shimadzu (Kyoto, Japan) HPLC system consisting of an LC-20ADXR binary pump, an SIL-20ACXR autosampler, a CTO-10AS VP column oven and an SPD-20A. Chromatographic separation of analytes was achieved using a DIKMA Diamonsil C18（4.6 mm × 250 mm, 5 μm）analytical column (DIKMA, Beijing, China). The column and autosampler tray temperatures were set at 30 and 4℃, respectively.

A mobile phase composed of eluent A (0.1% formic acid in water, v/v) and B (acetonitrile) with a gradient elution was employed for the separation. The mobile phase was programmed as follows: an isocratic elution of 2%-4% B for the first 15 min, followed by a linear gradient elution of 4%-13% B from 15 to 25 min, 13%-18% B from 25 to 30 min, 18% B from 30 to 44 min, 18%-40% B from 44 to 53 min, 40%-100% B from 53 to 53.01 min. After holding the solvent composition of 100% B for the next 3 min, the gradient was returned to its starting conditions. The flow rate was 1.0 mL/min, and samples were detected by absorption at 280 nm and 330 nm, with an inject volume of 20 μL.

*2.5 Cell culture*

The immortalized human sebaceous (Yansheng Industrial Co., Ltd, Shanghai, China) gland cell line (Sebocytes) was used. Human keratinocytes (HaCaT) were obtained from Meisen Cell Technology Co., Ltd. Sebocytes and HaCaT cells were incubated in complete Dulbecco's modified Eagle's medium (DMEM; Meisen Cell Technology Co., Hangzhou, China) containing 100 U/mL penicillin, streptomycin (100 μg/mL), and 10% fetal bovine serum (FBS, TransGen Biotech, Beijing, China).

*2.6 Cell viability assay*

Cell viability was assessed through a standard CCK-8 assay (Vazyme). Sebocytes and HaCaT cells were subjected to drug treatment post-adherence to the dish bottom. Following a 24-hour incubation, 10% CCK-8 reagent was introduced into each well. After 2 hours of incubation at 37℃, the optical density was gauged at a wavelength of 450 nm using a SpectraMax 190 plate reader (Molecular Devices Corporation, CA). The outcomes were expressed as relative to the control.

*2.7 Nile red staining*

Sebocytes were treated with Nile red to visualize intracellular lipid deposition. Post Nile red staining for 10 minutes, along with DAPI staining for cell nuclei, the stained cells were examined using a fluorescence microscope (MShot, Wuhan, China). Additionally, Sebocytes were suspended in 500 μL Dulbecco's phosphate-buffered saline (DPBS, Sigma-Aldrich, Shanghai, PR China), and their fluorescence intensity was measured using a flow cytometer (FACScalibur, Becton Dickinson, San Josè, CA USA).

*2.8 Microbial cultivation*

*Propionibacterium acnes* (*P. acnes*) (ATCC 6919) was procured from the China Industrial Culture Preservation Centre (Beijing, China). *P. acnes* was cultured anaerobically in solid and liquid fortified Clostridium difficile medium (Hopebiol, Shandong, China) at 37˚C for 72 hours. This suspension was

heat-treated at 80˚C, and the resulting heat-killed bacteria were employed in a previously documented stimulation experiment[20]. The collected bacterial pellet was eventually suspended in serum-free medium, achieving a bacterial concentration of $1.2 \times 10^9$ CFU/mL.

*2.9 Intracellular ROS Detection Assay Intracellular*

ROS levels were assessed using 2′,7′-dichlorodihydrofluorescein diacetate (DCFH-DA) (Beyotime, Shanghai, China). DCFH-DA at 5 μmol/L was added to each well and incubated at 37 ℃ for 0.5 h. The cells were then washed with DPBS (Sigma-Aldrich), suspended, and analyzed using a CytoFLEX Flow cytometer.

*2.10 Mitochondrial membrane potential assay*

The mitochondrial membrane potential was assessed with the fluorescent probe JC-1 (Beyotime). JC-1 generates red fluorescence in mitochondria with normal membrane potentials by forming aggregates. Conversely, in damaged or depolarized mitochondria, JC-1 forms monomers that emit green fluorescence. Cells were exposed to DMEM containing 5 μmol/L JC-1 for 15 minutes at 37℃, and subsequent imaging was conducted using a fluorescence microscope (MShot).

*2.11 Real-time reverse transcriptase-polymerase chain reaction*

Total ribonucleic acid (RNA) was extracted from cells employing RNA-easy Isolation Reagent (Vazyme). Subsequently, RNA was reverse transcribed to complementary DNA (cDNA) using the HiScript III 1st Strand cDNA Synthesis Kit (+gDNA wiper) (Vazyme). For quantitative polymerase chain reaction (qPCR), ChamQ Universal SYBR qPCR Master Mix (Vazyme) containing a fluorescent dye was utilized. The RT-qPCR analysis was conducted on a real-time PCR Detection system (Bioer, Hangzhou, China). All primer sequences were sourced from GenScript (Nanjing, China) (Table 1).

**Table 1** The primer sequences.

| Genes | Forward primer | Reveres primer |
|---|---|---|
| β-actin | TGGCACCCAGCACAATGAA | CTAAGTCATAGTCCGCCTAGAAGCA |
| PPARγ | GCCAAGCTGCTCCAGAAAAT | TGATCACCTGCAGTAGCTGCA |
| SREBP-1 | GGAGCCATGGATTGCACTTT | TCAAATAGGCCAGGGAAGTCA |
| IL-6 | GCAGAAAACAACCTGAACCTT | ACCTCAAACTCCAAAAGACCA |
| IL-1α | CAATTGTATGGACTGCCCAAG | ATAGTTCTTAGTGCCGTGAGTT |

## 3. Result

*3.1 Characterization of the chemical compounds in PHG and the metabolites in BJJF*

The UPLC-Q-TOF-MS system was utilized to identify the chemical constituents in both PHG and BJJF (Figure 1a-b). Referring to a previous study[21], we identified a total of 38 compounds, with 30 of them being PhGs (Table 2). Specifically, we noted six compounds in BJJF (dehydrogenated decaffeoylacteoside, HT, HT-rha-glu, caffeic acid sulfate conjugation, caffeic acid, and hydroxylated verbascoside) frequently documented in research on PhGs metabolism in vivo. These compounds originate from the parent compound through processes such as hydroxylation, sulfonation, or ester bond breaking. Additionally, we observed a parent ion at 655.1873 and secondary ion fragments at 461.1666 and 179.0350. These ions are probably to

represent a double-hydroxylated compound of verbascoside (623.2018), which has not been previously found in literature or CAS SciFinder, potentially indicating a new class of compounds. The introduction of additional hydroxyl groups is a common strategy employed by nature to enhance the stability, solubility, and biological activities of these aromatic compounds[22]. For instance, oxidized resveratrol demonstrates enhanced pharmacological activities compared to resveratrol in areas such as tyrosinase inhibition[23], anti-glycosylation[24], and anti-tumor effects[25]. Furthermore, we observed increased peak areas of small molecule PhGs like cistanoside G, cistanoside I, cistanoside F, and cistanoside H following fermentation. In positive ionization mode, we identified two specific metabolites of *B. bassiana*—oosporein and beauvericin, which exhibits antioxidant[26] and antibacterial properties[27].

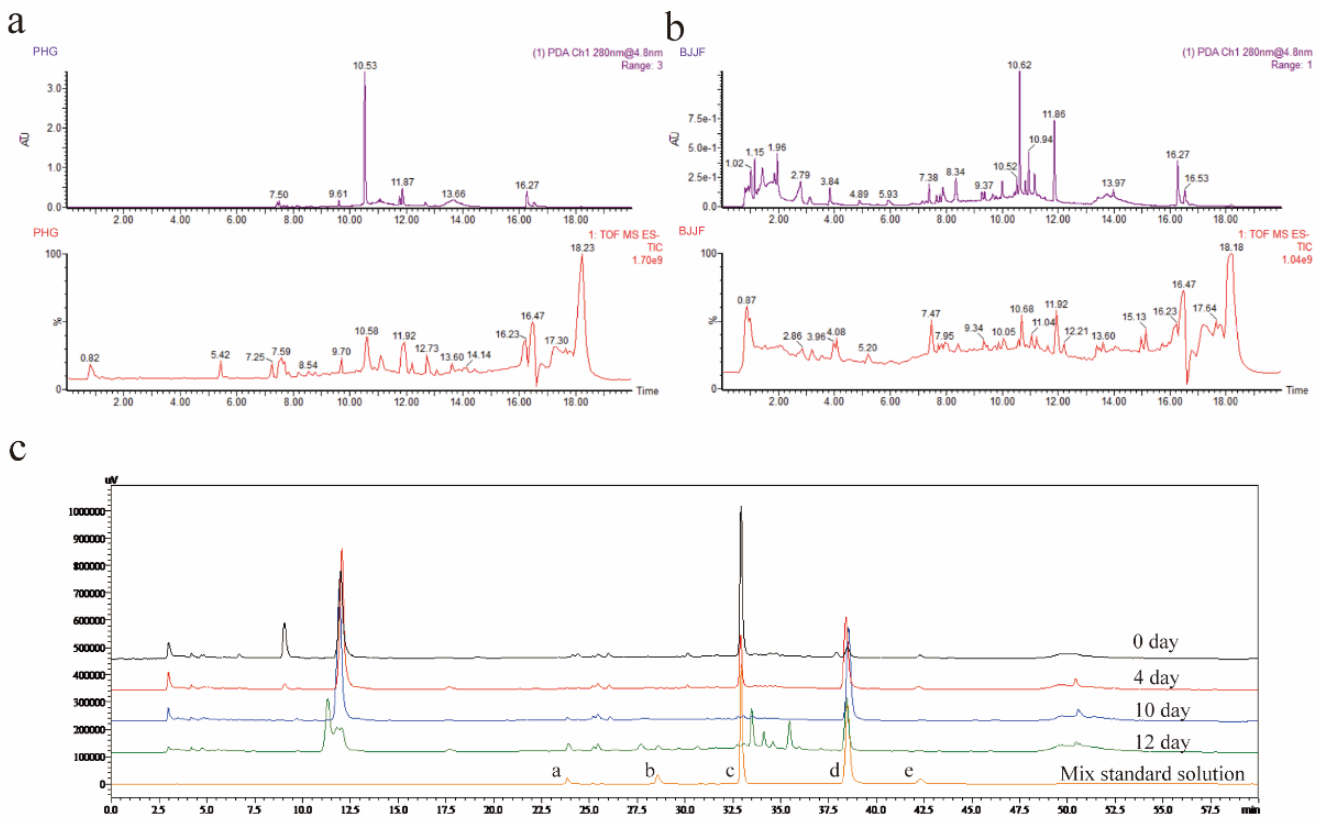


**Figure 1**. Total ion chromatograms and UPLC chromatogram at UV280 of PHG (a) and BJJF (b). (c) HPLC Chromatograms of *B. bassiana* fermentation crude extracts at different time points. In the mixed standard solution, the components are labeled as follows: a: HT-rha-glu, b: caffeic acid, c: echinacoside, d: verbascoside, e: isoacteoside.

**Table 2**. The compounds detected in PHG and BJJF by UPLC-Q-TOF-MS.

| No. | Compounds | RT (min) | Ion mode | m/z | Molecular formula | Error (ppm) | MS/MS fragments (m/z) | Peak area | |
|---|---|---|---|---|---|---|---|---|---|
| | | | | | | | | PHG | BJJF |
| 1 | Kankansose | 1.23 | [M-H]- | 649.1930 | $C_{27}H_{38}O_{18}$ | -8.47 | 305.0834,135.0460 | 8.2E+03 | 5.0E+05 |
| 2 | Dehydrogenated decaffeoylacteoside | 3.45 | [M-H]- | 459.1499 | $C_{20}H_{28}O_{12}$ | -1.96 | 151.0406 | 1.0E+06 | 6.0E+06 |
| 3 | Hydroxytyrosol | 4.67 | [M-H]- | 153.0555 | $C_8H_{10}O_3$ | -1.31 | 123.0449 | 0.0E+00 | 3.8E+06 |
| 4 | 6-deoxycatalpol | 7.47 | [M-H]- | 345.1189 | $C_{15}H_{22}O_9$ | -0.58 | 345.1183,299.1133 | 8.2E+07 | 1.8E+05 |
| 5 | HT-rha-glu | 7.47 | [M-H]- | 461.1696 | $C_{20}H_{30}O_{12}$ | 8.02 | 315.1089,153.0604 | 8.5E+06 | 3.1E+08 |
| 6 | Cistantubulose A1 | 7.54 | [M-H]- | 649.1983 | $C_{27}H_{38}O_{18}$ | -0.31 | 649.1985,623.2202,537.1812,335.0896,179.0360 | 2.2E+08 | 1.8E+06 |
| 7 | Adoxosidic acid | 7.71 | [M-H]- | 375.1298 | $C_{16}H_{24}O_{10}$ | 0.27 | 213.0768 | 8.5E+07 | 1.1E+06 |
| 8 | Caffeic acid sulfate conjugation | 8.00 | [M-H]- | 258.9926 | $C_9H_8O_7S$ | 3.09 | 167.0351,135.0451 | 2.6E+05 | 3.6E+08 |
| 9 | Androsin | 8.34 | [M-H]- | 327.1078 | $C_{15}H_{20}O_8$ | -2.14 | 251.0554,179.0349,131.0709 | 1.3E+06 | 9.3E+04 |
| 10 | Caffeic acid | 8.41 | [M-H]- | 179.0361 | $C_9H_8O_4$ | 6.14 | 134.0372 | 1.1E+07 | 2.2E+08 |
| 11 | Cistanoside G | 8.46 | [M-H]- | 445.1713 | $C_{20}H_{30}O_{11}$ | -0.45 | 375.1307,195.0685 | 1.2E+07 | 1.9E+07 |
| 12 | Cistanoside I | 8.93 | [M-H]- | 471.1507 | $C_{21}H_{28}O_{12}$ | -0.21 | 369.1104,163.0388 | 1.3E+06 | 7.8E+06 |
| 13 | Cistantubuloside C1 | 9.70 | [M-H]- | 801.2451 | $C_{35}H_{46}O_{21}$ | -1.00 | 251.0557,195.0656 | 1.8E+08 | 1.8E+06 |
| 14 | Hydroxylated Verbascoside | 10.46 | [M-H]- | 639.1931 | $C_{29}H_{36}O_{16}$ | 0.00 | 495.1504,179.0350 | 1.0E+08 | 8.6E+07 |
| 15 | Campneoside II | 10.51 | [M-H]- | 639.1929 | $C_{29}H_{36}O_{16}$ | -0.31 | 621.1827,461.1659,161.0250 | 1.0E+08 | 9.2E+07 |
| 16 | Echinacoside | 10.58 | [M-H]- | 785.2507 | $C_{35}H_{46}O_{20}$ | -0.38 | 785.2507,623.2158,153.0917 | 1.4E+08 | 8.4E+05 |
| 17 | Cistanoside F | 10.68 | [M-H]- | 487.1458 | $C_{21}H_{28}O_{13}$ | 0.21 | 179.0368,135.0452 | 1.0E+05 | 3.2E+07 |
| 18 | Dihydroxylated Verbascoside | 10.75 | [M-H]- | 655.1873 | $C_{29}H_{36}O_{17}$ | -1.07 | 487.1459,461.1666,179.0350 | 6.9E+05 | 6.7E+08 |
| 19 | Kankanosides K1/K2 | 11.09 | [M-H]- | 815.2610 | $C_{36}H_{48}O_{21}$ | -0.61 | 499.1815,197.7953 | 2.0E+07 | 2.1E+06 |
| 20 | Dihydroxylated Verbascoside | 11.22 | [M-H]- | 655.1874 | $C_{29}H_{36}O_{17}$ | -0.92 | 487.1455,323.0774,179.0350 | 2.1E+05 | 5.1E+08 |
| 21 | Kankanoside N | 11.56 | [M-H]- | 345.1551 | $C_{16}H_{26}O_8$ | -1.16 | 113.0234 | 4.9E+06 | 7.6E+04 |
| 22 | Crenatoside | 11.97 | [M-H]- | 621.1824 | $C_{29}H_{34}O_{15}$ | -0.16 | 461.1667,179.0349 | 1.5E+07 | 1.7E+07 |
| 23 | Verbascoside | 11.97 | [M-H]- | 623.2018 | $C_{29}H_{36}O_{15}$ | 5.94 | 469.1366,461.1667,315.1079,161.0245 | 2.8E+07 | 3.8E+08 |
| 24 | Kankanoside A | 11.97 | [M-H]- | 345.1554 | $C_{16}H_{26}O_8$ | -0.29 | 179.0349 | 1.9E+07 | 9.1E+04 |
| 25 | Isoacteoside | 12.73 | [M-H]- | 623.2008 | $C_{29}H_{36}O_{15}$ | 4.33 | 461.1662,161.0243 | 2.6E+07 | 1.7E+06 |
| 26 | Cistanoside H | 12.80 | [M-H]- | 503.1778 | $C_{22}H_{32}O_{13}$ | 1.59 | 461.1648,375.1361,315.0818 | 9.2E+03 | 5.7E+06 |
| 27 | Tubuloside A | 12.85 | [M-H]- | 827.2596 | $C_{37}H_{48}O_{21}$ | -2.30 | 623.1978,621.1821,469.1332,161.0243 | 8.3E+06 | 4.2E+04 |
| 28 | Campneoside | 13.43 | [M-H]- | 653.2092 | $C_{30}H_{38}O_{16}$ | 0.77 | 461.1673,443.1556,145.0296 | 4.4E+05 | 1.3E+07 |
| 29 | Isocistanoside C | 13.79 | [M-H]- | 637.2137 | $C_{30}H_{38}O_{15}$ | -0.16 | 179.0347,161.0242 | 3.7E+06 | 7.8E+06 |
| 30 | Isosyringalide 3'-alpha-L-rhamnopyranoside | 13.90 | [M-H]- | 607.2029 | $C_{29}H_{36}O_{14}$ | -0.49 | 461.1645,315.0911,145.0314 | 1.1E+07 | 3.8E+06 |
| 31 | Tubuloside B | 14.02 | [M-H]- | 665.2100 | $C_{31}H_{38}O_{16}$ | 1.95 | 503.1765,305.0670,161.0242 | 8.1E+07 | 1.4E+08 |
| 32 | Plantainoside C | 14.26 | [M-H]- | 637.2120 | $C_{30}H_{38}O_{15}$ | -2.82 | 445.1516,145.0291 | 2.5E+06 | 1.1E+06 |
| 33 | 2′-acetylacteoside | 14.43 | [M-H]- | 665.2084 | $C_{31}H_{38}O_{16}$ | -0.45 | 503.1763,161.0242 | 7.2E+07 | 4.3E+06 |
| 34 | SalsasideF | 14.55 | [M-H]- | 649.2131 | $C_{31}H_{38}O_{15}$ | -1.08 | 503.1754,347.1670,161.0243 | 3.4E+06 | 2.2E+07 |
| 35 | Osmanthuside B6 | 15.13 | [M-H]- | 591.2080 | $C_{29}H_{36}O_{13}$ | -0.51 | 161.0237 | 3.9E+06 | 1.9E+07 |
| 36 | Eutigoside A | 16.13 | [M-H]- | 445.1534 | $C_{23}H_{26}O_9$ | 6.74 | 145.0305,163.0416 | 3.3E+06 | 7.9E+05 |
| 37 | Oosporein | 1.52 | [M+Na]+ | 329.0296 | $C_{14}H_{10}O_8$ | 8.51 | 254.0249 | 0.0E+00 | 2.0E+04 |
| 38 | Beauvericin | 10.63 | [M+K]+ | 822.3723 | $C_{45}H_{57}N_3O_9$ | -0.36 | 663.3060,262.1499,245.1370,244.1306,134.0965 | 0.0E+00 | 1.4E+04 |

*3.2 Analysis of metabolic pathways and the contents of compounds in the BJJF*

The results from our sampling at different time points to analyze substance content in the samples are presented in Table 3. In the initial fermentation stage, spanning from 0 to 6 days, we observed the conversion of echinacoside into verbascoside, indicating the presence of robust glucosidase in the culture broth. Simultaneously, a fraction of verbascoside and isoacteoside transformed into HT-rha-glu and caffeic acid. In the later stage, from 6 to 12 days, verbascoside underwent partial hydroxylation and partial transformation into HT-rha-glu and caffeic acid (Figure 1c). The unequal presence of HT-rha-glu and caffeic acid is due to the sulfation of caffeic acid in one portion, possibly accompanied by partial oxidation during fermentation. The fermentation progression is illustrated in Figure 2.

**Table 3**. The contents of compounds and metabolites in BJJF with *Beauveria bassiana* at different time points ($n$ = 5).

| Conmpound | Concentration (μg/mL) | | | | | | |
|---|---|---|---|---|---|---|---|
| | 0 day | 2 day | 4 day | 6 day | 10 day | 11 day | 12 day |
| HT-rha-glu | <LOD | <LOD | 11.313 ±0.748 | 15.239 ±0.896 | 27.524 ±2.371 | 53.150 ±3.278 | 75.030 ±2.393 |
| Caffeic acid | <LOD | <LOD | <LOD | <LOD | <LOD | 5.395 ±0.609 | 8.104 ±0.176 |
| Echinacoside | 346.389 ±12.915 | 251.963 ±11.096 | 97.738 ±10.954 | <LOD | <LOD | <LOD | <LOD |
| Verbascoside | 32.559 ±1.186 | 120.310 ±8.067 | 246.452 ±17.087 | 316.568 ±15.073 | 307.057 ±9.294 | 228.559 ±3.194 | 158.846 ±3.545 |
| Isoacteoside | 14.256 ±0.614 | 15.797 ±0.580 | 13.985 ±0.446 | 10.585 ±0.896 | <LOD | <LOD | <LOD |

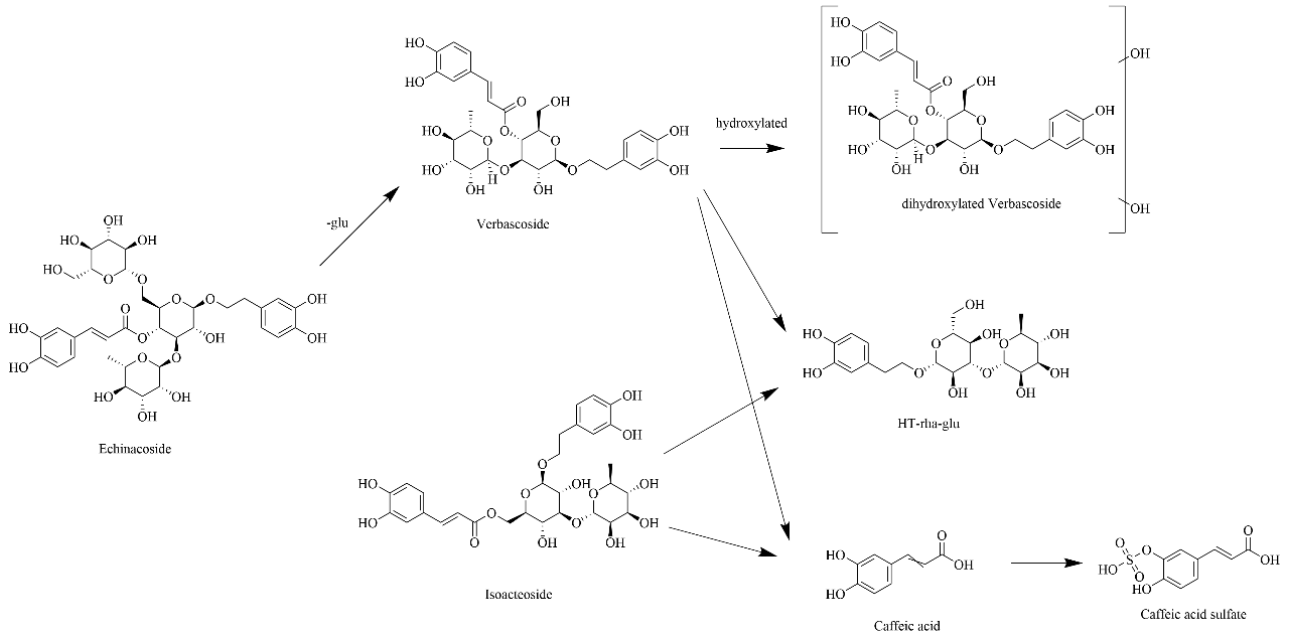


**Figure 2**. Clarifications on the metabolic pathways of echinacoside, verbascoside, and isoacteoside.

*3.3 Effects of PHG and BJJF on P. acnes-stimulated HaCaT cells*

HaCaT cell viability was assessed using CCK8 after 24 hours of incubation with either PHG or BJJF. The increased dosage of PHG/BJJF (0.5%-2% (v/v)) didn't result in significant changes (Figure 3a). *P. acnes* plays a key role in acne's development, initiating inflammation by triggering ROS production and

releasing inflammatory cytokines[28]. HaCaT cells were cultured in 6-well plates and treated with PHG or BJJF, with or without *P. acnes*, for 24 hours. Figures 3b-c illustrate that both PHG and BJJF at dosages of 0.5%-1% (v/v) reduced the gene expression of *P. acnes*-induced inflammatory factors IL-1α and IL-6 in a dose-dependent manner. Notably, the 0.25%-0.5% dose of BJJF was more effective than the 0.25%-0.5% dose of PHG in inhibiting IL-1α gene expression. Analyses of green fluorescence intensity via flow cytometry showed that both PHG and BJJF reduced ROS production in *P. acnes*-stimulated HaCaT cells. BJJF exhibited superior performance in reducing ROS at all doses, notably at 1% (Figure 3d). Moreover, JC-1 staining indicated that both PHG and BJJF prevented the decline in mitochondrial membrane potential induced by *P. acnes* (Figure 3e).

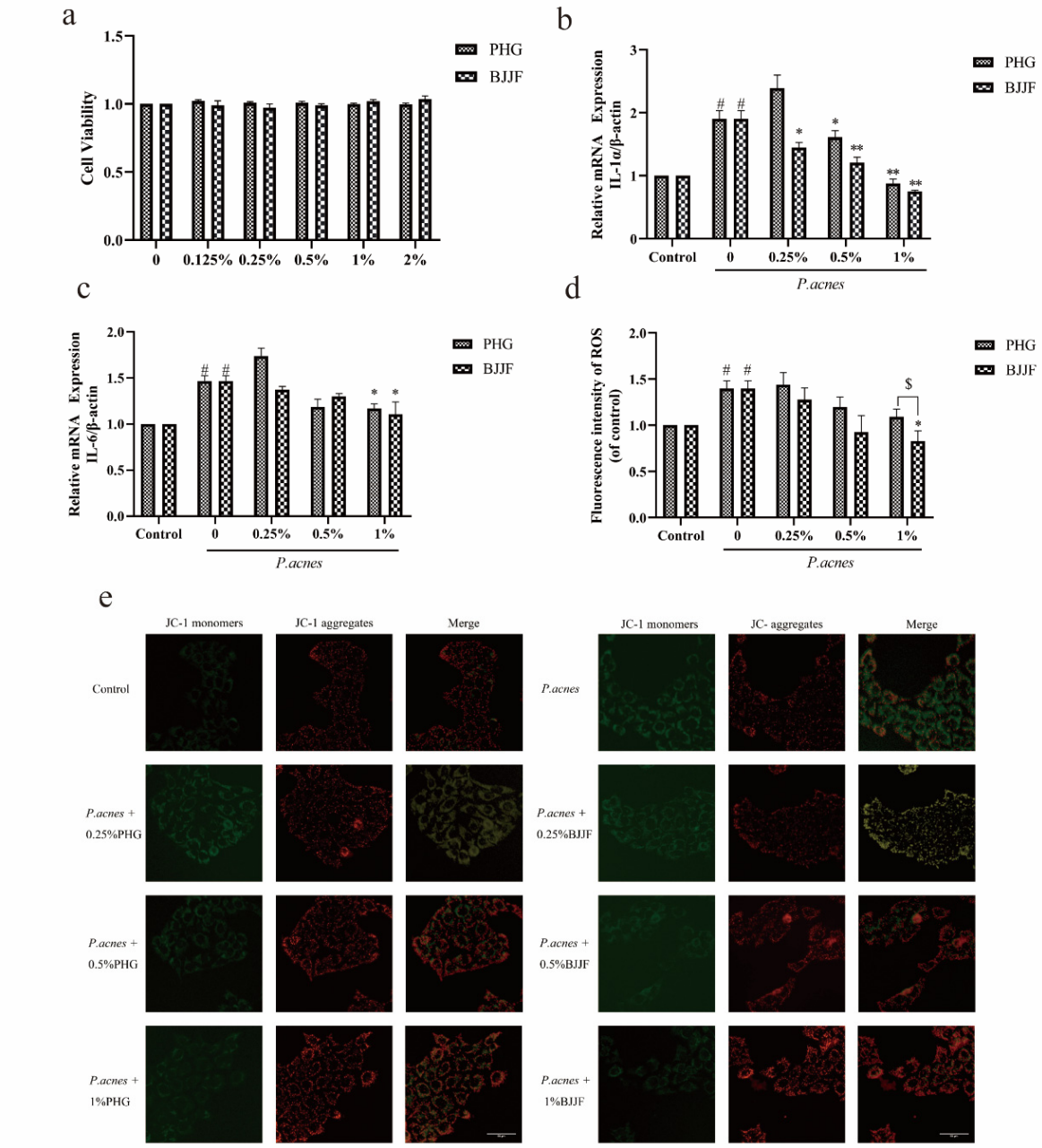


**Figure 3.** PHG and BJJF reduce the damage caused by *P. acnes* to HaCaT cells. (a) Cell viability was determined by CCK8 assay. (b-c) The mRNA expression of IL-1α and IL-6 was detected using RT-qPCR. (d) ROS levels were quantified as mean fluorescence intensity relative to that in the control group. (e) JC-1 staining was used for assessing mitochondrial membrane potential. Scale bar = 50 μm. All data were expressed as means ± SEM (n=3). $^{\#}P < 0.05$ *vs.* control group, $^{*}P < 0.05$ and $^{**}P < 0.01$ *vs. P. acnes*-induced group, $^{\$}P < 0.05$ *vs.* 1% PHG group.

### *3.4 Effects of BJJ and HT-rha-glu on P. acnes-stimulated HaCaT cells*

The increased dosage of BJJ (0.25%-1% (v/v)) did not result in significant changes in cell viability, as measured by CCK8, after 24 hours of incubation with HaCaT cells (Figure 4a). In HaCaT cells stimulated by *P. acnes*, there was a tendency for ROS production and the expression of IL-1α and IL-6 genes to decrease with increasing BJJ concentration, although this decrease was not statistically significant (Figure 4b-d). The cell viability of HaCaT was unaffected by 0.75-12 μg of HT-rha-glu (Figure 4e). HT-rha-glu dose-dependently reduced ROS production, as well as IL-1α and IL-6 gene expression in HaCaT cells stimulated by *P. acnes* (Figure 4f-h).

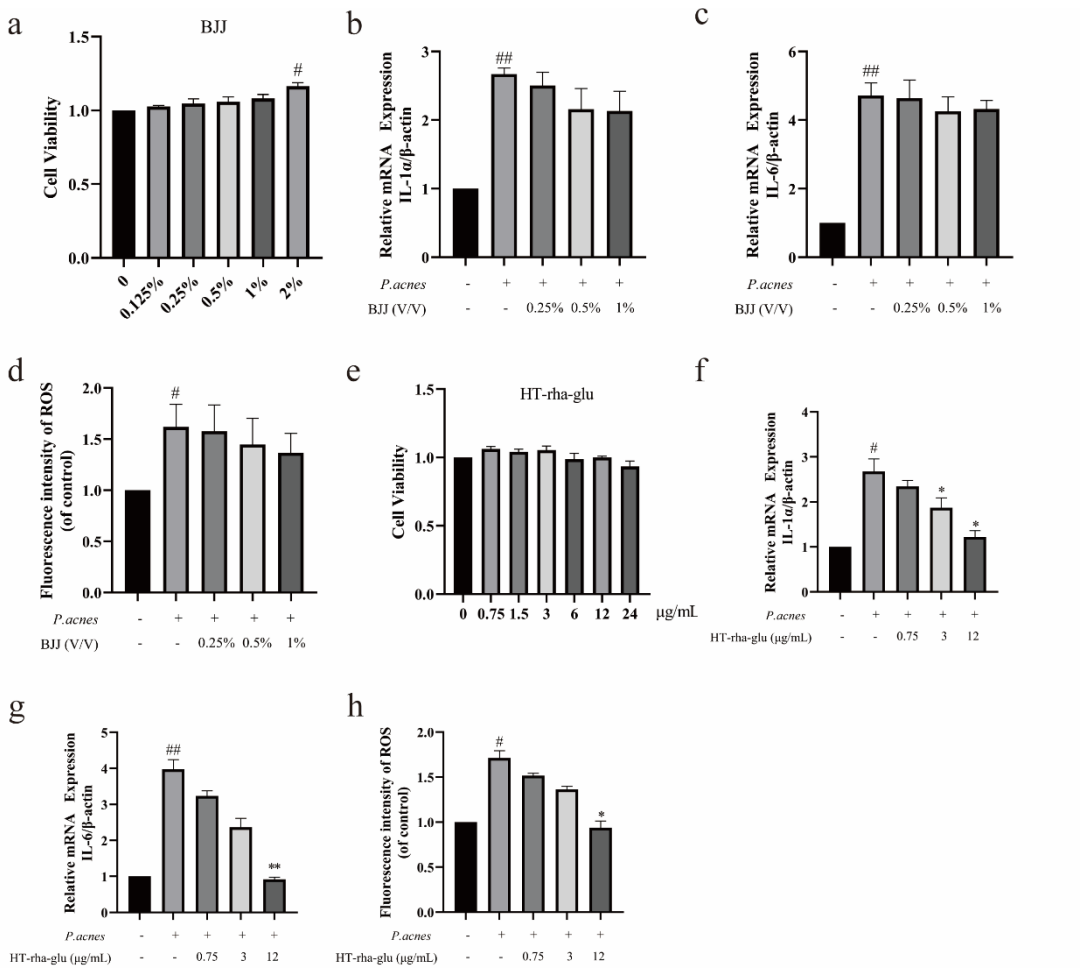


**Figure 4.** BJJ and HT-rha-glu exert effects on *P. acnes*-stimulated HaCaT cells. Cell viability after BJJ (a) and HT-rha-glu (e) treatment was determined by the CCK8 assay. The mRNA expression of IL-1α and IL-6 was detected using RT-qPCR after BJJ (b-c) and HT-rha-glu (f-g) treatments. ROS levels were quantified as mean fluorescence intensity relative to that in the control group using flow cytometry after treatments with BJJ (d) and HT-rha-glu (h). All data were expressed as means ± SEM (n=3). $^{\#}P < 0.05$ and $^{\#\#}P < 0.01$ *vs.* control group, $^{*}P < 0.05$ and $^{**}P < 0.01$ *vs. P. acnes*-induced group.

### *3.5 Effects of PHG and BJJF on insulin-stimulated sebocytes*

Sebocytes' survival was evaluated using the CCK8 assay after 24 hours of incubation with either PHG or BJJF. Different concentrations of PHG/BJJF (ranging from 0.5% to 2% (v/v)) didn't exhibit significant changes (Figure 5a). While examining cytofluorescence using Nile Red dye, a significant increase in the count of intracellular lipid droplets was noted after 24 hours of insulin treatment. BJJF (concentrations ranging from 0.5% to 1% (v/v)) displayed a concentration-dependent inhibition of insulin-induced

lipogenesis. However, PHG did not exhibit an inhibition of insulin-induced lipogenesis (Figure 5b). The fluorescence microscopy, which involved co-staining with Nile Red and DAPI, produced consistent results as observed in flow cytometry (Figure 5c).

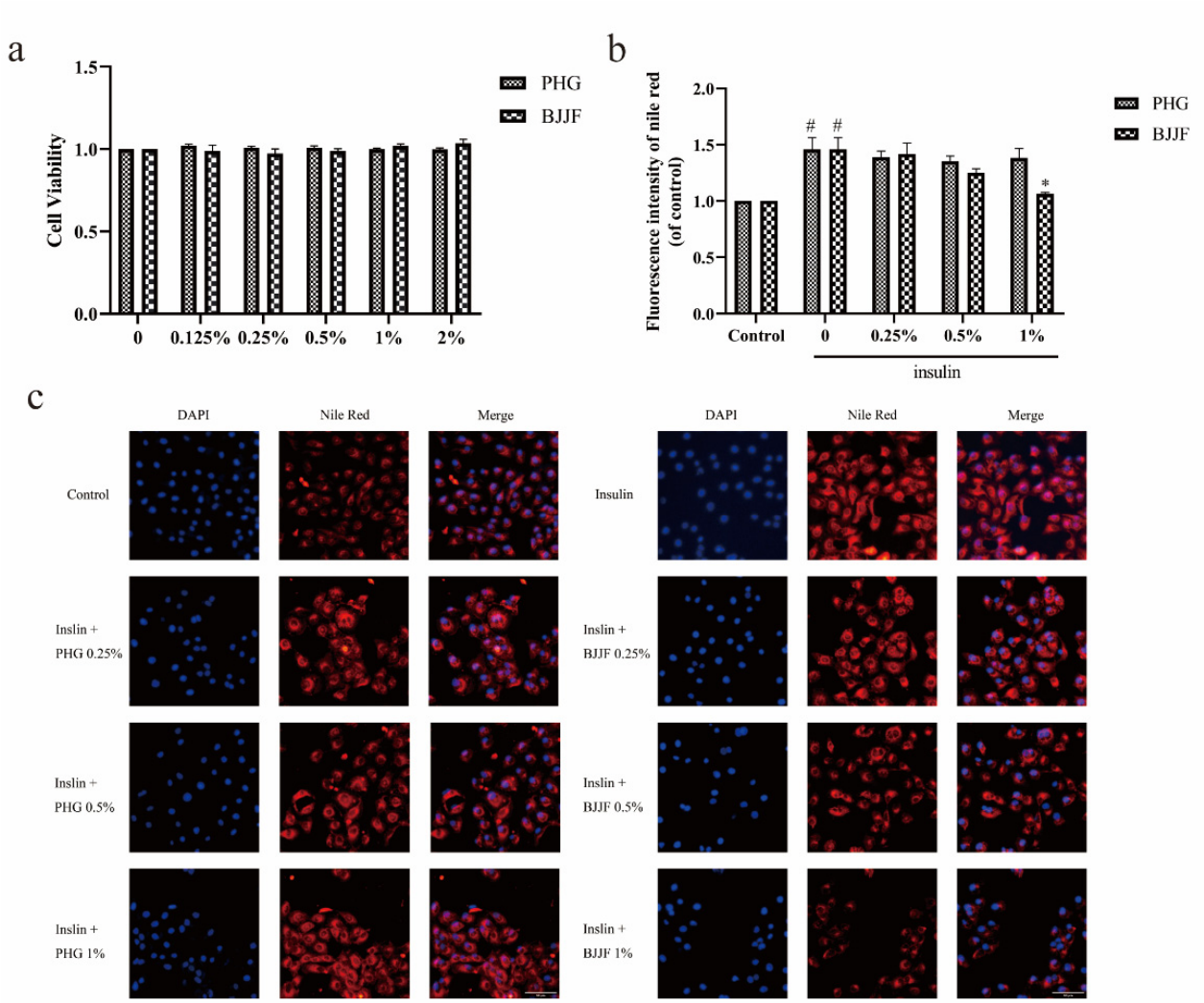


**Figure 5.** PHG and BJJF's impact on insulin-induced lipid synthesis in sebaceous gland cells. (a) Cell viability was determined by CCK8 assay. (b) Using a flow cytometer, the neutral lipid contents were determined after being stained with Nile red. (c) Red fluorescence indicates neutral lipids stained with Nile red, and blue fluorescence indicates the position of cell nuclei stained with DAPI. All data were expressed as means ± SEM (n=3). $^{\#}P < 0.05$ *vs.* control group, $^{*}P < 0.05$ *vs.* insulin-stimulated group.

### *3.6 Impact of HT-rha-glu on insulin-stimulated sebocytes and an exploration of the underlying mechanism*

The cell viability of sebocytes was unaffected by 0.75-12 μg of HT-rha-glu and 0.25%-1% of BJJ (Figure 6a and c). HT-rha-glu, a compound largely generated by the fermentation. From the structure point of view, HT-rha-glu incorporates a rhamnose and a glucose into the HT core, enhancing HT's stability to a certain extent. Our research indicates that HT-rha-glu, within the range of 0.75-12 μg/mL, can dose-dependently reduce sebocyte lipid synthesis, unlike BJJ (Figure 6b and d). Through real-time PCR, we observed that HT-rha-glu treatment led to a dose-dependent decrease in the gene expression of SREBP-1 and PPARγ in comparison to insulin-treated sebocytes (Figure 6e-f). This could explain that the post-fermentation enhanced the effect of inhibiting insulin-stimulated lipid synthesis in sebaceous gland cells.

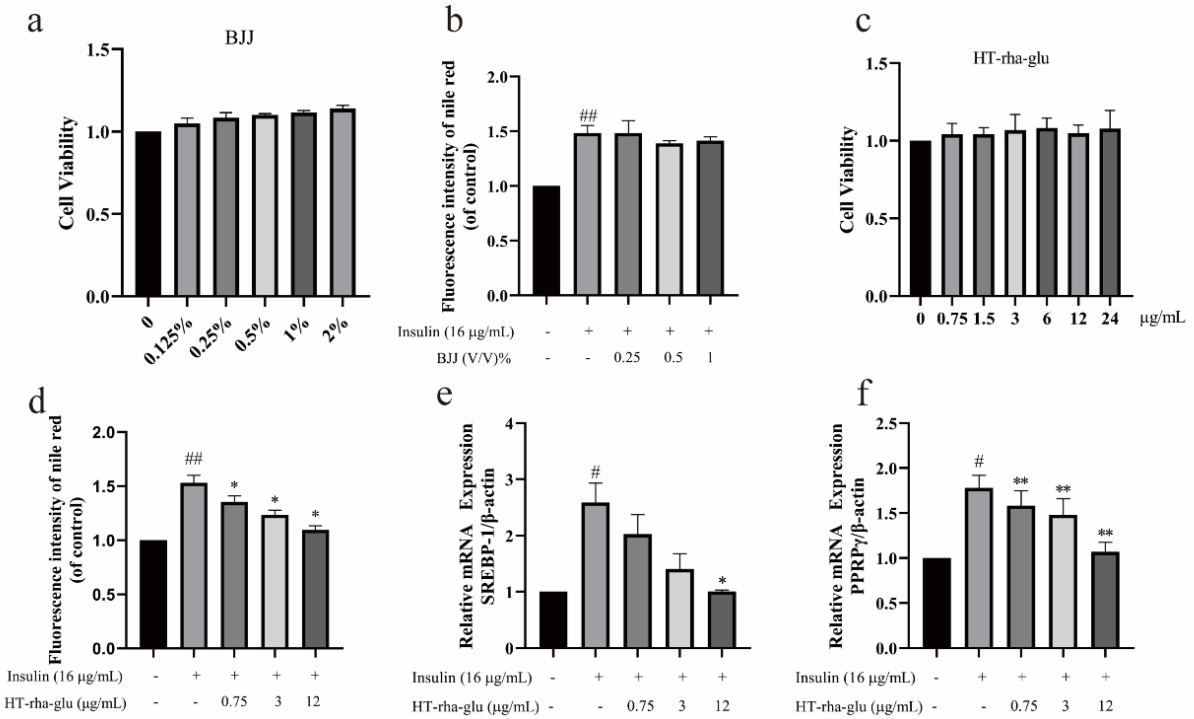


**Figure 6.** HT-rha-glu inhibited insulin-induced lipid synthesis in sebocytes. Cell viability after BJJ (a) and HT-rha-glu (c) treatment was determined by the CCK8 assay. Neutral lipid contents were measured by flow cytometry after BJJ (b) and HT-rha-glu (d) treatments. RT-qPCR was conducted to measure the mRNA levels of SREBP-1 (e) and PPARγ (f) in insulin-induced lipid synthesis in sebaceous gland cells after HT-rha-glu treatment. All data were expressed as means ± SEM (n=3). $^{\#}P < 0.05$ and $^{\#\#}P < 0.01$ *vs.* control group, $^{*}P < 0.05$ and $^{**}P < 0.01$ *vs.* insulin-stimulated group.

## 4. Discussion:

The benefits of fermented foods and herbs for overall systemic health are increasingly evident, backed by a growing body of evidence across various studies. Fermentation has the potential to generate and enrich a wide range of bioactive compounds. This process, driven by microorganisms, not only amplifies the original traits of the food but also introduces novel effects or properties[29].

In our research, we've made a novel discovery—during fermentation, the medicinal fungus *B. bassiana* transforms PhGs from Cistanche herbs into smaller polyphenols. The fermentation process occurs in stages: echinacoside is transformed into verbascoside, followed by the metabolism of a portion of verbascoside into HT-glu-rha and caffeic acid, with the latter converting into sulfation of caffeic acid. HT, the mother nucleus structure of HT-glu-rha, is widely recognized as an exceptional antioxidant compound sourced from plants. It possesses anti-inflammatory properties, aids in combating Alzheimer's disease, and inhibits liver lipid synthesis. This component plays a pivotal role in Cistanche's internal metabolism, exerting its medicinal effects. Indeed, while HT itself is quite unstable, HT-glu-rha demonstrates a similar activity to HT while maintaining greater stability, owing to the glycosidic bond linkage. However, studies on the pharmacological activity and pharmacokinetics of HT-glu-rha are quite limited, and we will explore this in more depth in a subsequent study. Interestingly, some of verbascoside was hydroxylated, indicating the potential presence of cytochrome P450 enzymes or polyphenol oxidase in the fermentation broth. This aligns with the *in vivo* metabolism pattern of PhGs, leading to the formation of hydroxylated components[11, 30].

PhGs undergo multiple routes of hydrolysis in the gastrointestinal tract and produce degradation intermediates before being absorbed into the blood[31, 32]. Indeed, each individual possesses a unique microbiota composition, impacting the bioavailability of PhGs and subsequent production of microbial metabolites, leading to interindividual variability in health effects. Consequently, these effects may not be uniform for everyone. For the first time, we conducted *in vitro* biotransformation of the PhGs, aligning with their metabolism *in vivo*. This process holds the potential to address the variability in the effects of PhGs observed in different individuals.

Acne vulgaris is one of the most common dermatologic conditions globally which is closely related to Western diet[33]. Diet-triggered insulin or insulin-like growth factor activation of the mammalian target of rapamycin complex 1 (mTORC1) is associated with acne. mTORC1 is responsible for sebaceous gland hyperproliferation, lipid synthesis, and keratinocyte hyperplasia in acne cases[34]. *P. acnes* flourishes when sebum production increases[35]. It triggers inflammatory responses by stimulating the production of molecules associated with inflammation, including TLR, MMP, and inflammatory cytokines[36]. Our research revealed that heat-killed *P. acnes* irritated HaCaT increased IL-1α and IL-6 expression, while PHG and BJJF showed a dose-dependent suppression of these cytokines in the HaCaT cells. Interestingly, higher doses of BJJF exhibited notably superior effects in reducing ROS production induced by *P. acnes* in HaCaT cells, possibly due to the increased likelihood of small-molecule polyphenols to penetrate cell membranes and exert biological activities. Moreover, in insulin-stimulated sebocytes, unlike PHG, BJJF demonstrated a dose-dependent reduction in lipid synthesis. Additionally, HT-rha-glu exhibited similar reductions in lipid synthesis in insulin-stimulated sebocytes by down-regulating the gene expression of SREBP-1 and PPARγ in a dose-dependent manner. However, further studies such as toxicological and pharmacokinetic on our samples are needed before they can be developed into active materials for topical or oral use. In addition, although we performed the fermentation in laboratory conical flasks, further experimental scale-up is required to assess its potential for industrial production.

## 5. Conclusions

Fermentation of Cistanche extract by *B. bassiana* metabolized the PhGs into small polyphenols, especially HT-rha-glu, enhancing its antioxidant and lipid inhibitory activities. Given the potent bioenzymatic activity of *B. bassiana,* it would be worthwhile to further explore its use in the fermenting hard-to-absorb foods and herbs to enhance their activity and utilization.

## Declaration of competing interest

No conflict of interest exits in the submission of this manuscript, and manuscript is approved by all authors for publication, the work described was original research that has not been published previously, and not under consideration for publication elsewhere, in whole or in part.

## Acknowledgments

This research was supported by the start-up fund of China Pharmaceutical University.

## References


[1] H.M. Shi, J. Wang, M.Y. Wang, et al., Identification of Cistanche Species by Chemical and Inter-simple Sequence Repeat Fingerprinting, Biol Pharm Bull. 32 (2009) 142-146. https://doi.org/10.1248/bpb.32.142.

[2] K.W. Zeng, J.K. Wang, L.C. Wang, et al., Small molecule induces mitochondrial fusion for neuroprotection via targeting CK2 without affecting its conventional kinase activity, Signal Transduct Target Ther. 6 (2021) 71. https://doi.org/10.1038/s41392-020-00447-6.

[3] S. Tian, M.S. Miao, X.M. Li, et al., Study on neuroendocrine-immune function of Phenylethanoid Glycosides of Desertliving Cistanche herb in perimenopausal rat model, J Ethnopharmacol. 238 (2019) 111884. https://doi.org/10.1016/j.jep.2019.111884.

[4] K. Zhang, X. Ma, W. He, et al., Extracts of Cistanche deserticola Can Antagonize Immunosenescence and Extend Life Span in Senescence-Accelerated Mouse Prone 8 (SAM-P8) Mice, Evid Based Complementary Altern Med. 2014 (2014) 601383. https://doi.org/10.1155/2014/601383.

[5] L. Yang, S. Ding, B. Zhang, et al., Beneficial Effects of Total Phenylethanoid Glycoside Fraction Isolated from Cistanche deserticola on Bone Microstructure in Ovariectomized Rats, Oxid Med Cell Longev. 2019 (2019) 2370862. https://doi.org/10.1155/2019/2370862.

[6] D. Feng, S.Q. Zhou, Y.X. Zhou, et al., Effect of total glycosides of Cistanche deserticola on the energy metabolism of human HepG2 cells, Front Nutr. 10 (2023) 1117364. https://doi.org/10.3389/fnut.2023.1117364.

[7] Y. Jiang, P.F. Tu, Analysis of chemical constituents in Cistanche species, J Chromatogr A. 1216 (2009) 1970-1979. https://doi.org/10.1016/j.chroma.2008.07.031.

[8] C. Jia, H. Shi, X. Wu, et al., Determination of echinacoside in rat serum by reversed-phase high-performance liquid chromatography with ultraviolet detection and its application to pharmacokinetics and bioavailability, J Chromatogr B. 844 (2006) 308-313. https://doi.org/10.1016/j.jchromb.2006.07.040.

[9] J.K. Nicholson, E. Holmes, I.D. Wilson, Gut microorganisms, mammalian metabolism and personalized health care, Nat Rev Microbiol. 3 (2005) 431-438. https://doi.org/10.1038/nrmicro1152.

[10] Y. Li, G. Zhou, S. Xing, et al., Identification of Echinacoside Metabolites Produced by Human Intestinal Bacteria Using Ultraperformance Liquid Chromatography-Quadrupole Time-of-Flight Mass Spectrometry, J Agric Food Chem. 63 (2015) 6764-6771. https://doi.org/10.1021/acs.jafc.5b02881.

[11] Y. Wang, H. Hao, G. Wang, et al., An approach to identifying sequential metabolites of a typical phenylethanoid glycoside, echinacoside, based on liquid chromatography-ion trap-time of flight mass spectrometry analysis, Talanta. 80 (2009) 572-580. https://doi.org/10.1016/j.talanta.2009.07.027.

[12]Q. Cui, Y. Pan, X. Xu, et al., The metabolic profile of acteoside produced by human or rat intestinal bacteria or intestinal enzyme in vitro employed UPLC-Q-TOF-MS, Fitoterapia. 109 (2016) 67-74. https://doi.org/10.1016/j.fitote.2015.12.011.

[13]Q. Xu, X. Fang, D. Chen, Pharmacokinetics and bioavailability of ginsenoside Rb1 and Rg1 from Panax notoginseng in rats, J Ethnopharmacol. 84 (2003) 187-192. https://doi.org/10.1016/s0378-8741(02)00317-3.

[14] A. König, N. Sadova, M. Dornmayr, et al., Combined acid hydrolysis and fermentation improves bioactivity of citrus flavonoids in vitro and in vivo, Commun Biol. 6 (2023) 1083. https://doi.org/10.1038/s42003-023-05424-7.

[15] M. Hu, Z. Yu, J. Wang, et al., Traditional Uses, Origins, Chemistry and Pharmacology of Bombyx batryticatus: A Review, Molecules. 22 (2017) 1779. https://doi.org/10.3390/molecules22101779.

[16] G. Zimmermann, Review on safety of the entomopathogenic fungiBeauveria bassianaandBeauveria brongniartii, Biocontrol Sci Technol. 17 (2007) 553-596. https://doi.org/10.1080/09583150701309006.

[17] L. Qiao, D. Xie, Q. Liu, et al., Microbial transformation of lovastatin by Beauveria bassiana, Acta Pharm Sin B. 2 (2012) 300-305. https://doi.org/https://doi.org/10.1016/j.apsb.2012.04.001.

[18] Q. Wu, J. Patocka, K. Kuca, Beauvericin, A Fusarium Mycotoxin: Anticancer Activity, Mechanisms, and Human Exposure Risk Assessment, Mini Rev Med Chem. 19 (2019) 206-214. https://doi.org/10.2174/1389557518666180928161808

[19] C. Rabhi, G. Arcile, L. Cariel, et al., Antiangiogenic-Like Properties of Fermented Extracts of Ayurvedic Medicinal Plants, J Med Food. 18 (2015) 1065-1072. https://doi.org/10.1089/jmf.2014.0128.

[20] Y.Y. Wang, A.R. Ryu, S. Jin, et al., Chlorin e6-Mediated Photodynamic Therapy Suppresses P. acnes-Induced Inflammatory Response via NFκB and MAPKs Signaling Pathway, PLOS ONE. 12 (2017) e0170599. https://doi.org/10.1371/journal.pone.0170599.

[21] Z. Li, L. Ryenchindorj, B. Liu, et al., Chemical profiles and metabolite study of raw and processed Cistanche deserticola in rats by UPLC-Q-TOF-MSE, Chinese Med. 16 (2021) 93. https://doi.org/10.1186/s13020-021-00508-0.

[22] R. Ullrich, M. Hofrichter, Enzymatic hydroxylation of aromatic compounds, Cell Mol Life Sci. 64 (2007) 271-293. https://doi.org/10.1007/s00018-007-6362-1.

[23] H.J. Zeng, Q.Y. Li, J. Ma, et al., A comparative study on the effects of resveratrol and oxyresveratrol against tyrosinase activity and their inhibitory mechanism, Spectrochim Acta A Mol Biomol Spectrosc. 251 (2021) 119405. https://doi.org/10.1016/j.saa.2020.119405.

[24] W. Wang, R. Yang, H. Yao, et al., Inhibiting the formation of advanced glycation end-products by three stilbenes and the identification of their adducts, Food Chem. 295 (2019) 10-15. https://doi.org/10.1016/j.foodchem.2019.02.137.

[25] Y. Yang, G. Zhang, C. Li, et al., Metabolic profile and structure-activity relationship of resveratrol and its analogs in human bladder cancer cells, Cancer Manag Res. 11 (2019) 4631-4642. https://doi.org/10.2147/cmar.S206748.

[26] L. Hu, X. Sui, X. Dong, et al., Low beauvericin concentrations promote PC-12 cell survival under oxidative stress by regulating lipid metabolism and PI3K/AKT/mTOR signaling, Ecotoxicol Environ Saf. 269 (2024) 115786. https://doi.org/10.1016/j.ecoenv.2023.115786.

[27] Y. Fan, X. Liu, N. Keyhani, et al., Beauveria bassianaRegulatory cascade and biological activity of oosporein that limits bacterial growth after host death, Proc Natl Acad Sci U.S.A. 114 (2017) E1578-E1586. https://doi.org/10.1073/pnas.1616543114.

[28] A. Jain, E. Basal, Inhibition of Propionibacterium acnes-induced mediators of inflammation by Indian herbs, Phytomedicine. 10 (2003) 34-38. https://doi.org/https://doi.org/10.1078/094471103321648638.

[29] A. Mukherjee, S. Breselge, E. Dimidi, et al., Fermented foods and gastrointestinal health: underlying mechanisms, Nat Rev Gastroenterol Hepatol. 4 (2023) 248-266. https://doi.org/10.1038/s41575-023-00869-x.

[30] H. Qian, F.J. Yu, D.Y. Lu, et al., Identification of poliumoside metabolites in rat plasma, urine, bile, and intestinal bacteria with UPLC/Q-TOF-MS, Chin J Nat Med. 16 (2018) 871-880. https://doi.org/10.1016/s1875-5364(18)30129-8.

[31] S. Hurst, C.M. Loi, J. Brodfuehrer, et al., Impact of physiological, physicochemical and biopharmaceutical factors in absorption and metabolism mechanisms on the drug oral bioavailability of rats and humans, Expert Opin Drug Metab Toxicol. 3 (2007) 469-489. https://doi.org/10.1517/17425225.3.4.469.

[32] Y. Li, Y. Peng, M. Wang, et al., Rapid screening and identification of the differences between metabolites of Cistanche deserticola and C. tubulosa water extract in rats by UPLC-Q-TOF-MS combined pattern recognition analysis, J Pharm Biomed Anal. 131 (2016) 364-372. https://doi.org/10.1016/j.jpba.2016.09.018.

[33] L. Cordain, S. Lindeberg, M. Hurtado, et al., Acne vulgaris: a disease of Western civilization, Arch Dermatol. 138 (2002) 1584-1590. https://doi.org/10.1001/archderm.138.12.1584.

[34] B. Melnik, Dietary intervention in acne: Attenuation of increased mTORC1 signaling promoted by Western diet, Dermatoendocrinol. 4 (2012) 20-32. https://doi.org/10.4161/derm.19828.

[35] K.J. McGinley, G.F. Webster, M.R. Ruggieri, et al., Regional variations in density of cutaneous propionibacteria: correlation of Propionibacterium acnes populations with sebaceous secretion, J Clin Microbiol. 12 (1980) 672-675. https://doi.org/10.1128/jcm.12.5.672-675.1980.

[36] J. Kim, Review of the innate immune response in acne vulgaris: activation of Toll-like receptor 2 in acne triggers inflammatory cytokine responses, Dermatology. 211 (2005) 193-198. https://doi.org/10.1159/000087011.